J Mater Sci: Mater Med (2009) 20:287–294
DOI 10.1007/s10856-008-3571-6

Incorporation of bovine serum albumin into biomimetic coatings on titanium with high loading efficacy and its release behavior

Xiaohua Yu · Haibo Qu · David A. Knecht · Mei Wei

Received: 15 April 2008 / Accepted: 18 August 2008 / Published online: 3 September 2008

Abstract Bovine serum albumin (BSA) was employed as a model protein to study its loading efficiency into a calcium phosphate (CaP) coating on titanium substrates. It is found that the protein loading efficiency can be adjusted by varying the specific configurations of the coating system such as simulated body fluid (SBF) volume, solution height and container selection for the SBF. A BSA loading efficiency as high as 90% was achieved when the ratio of the substrate surface area to modified SBF (m-SBF) volume was as high as 0.072. The release of BSA from the biomimetic coatings was also investigated in vitro. A sustained release was achieved although a large quantity of BSA was still trapped in the coating after 15 days of immersion in a phosphate buffer solution. A much faster release rate would be expected when the coating is implanted in vivo due to the active involvement of osteoclast cells and enzymes.

1 Introduction

Biomimetic coating has been developed for more than 15 years to improve the biological performance of biomaterials since Kokubo first introduced the coating method by soaking biomaterials in a simulated body fluid (SBF) with ion concentrations similar to human blood plasma [1]. Compared to other coating techniques, biomimetic coating has certain advantages. It is conducted at a temperature which is close to body temperature (37°C) and pH (7.4) [2]. Biologically active molecules, such as growth factors, can be co-precipitated with CaP crystals onto the surface of the metal implants without compromising the bioactivity of osteogenenic agents due to the mild conditions employed during the coating process [3]. It has been reported that the CaP coatings incorporated with bioactive molecules can substantially improve the bioactivity [3–5] and enhance the osteogenic activity of the implant [6–8].

Although biomimetic CaP coatings have been found to offer significant improvement in the bonding between implants and natural tissue, it still does not meet all clinical requirements such as adequate new bone formation on the healing site [6]. To overcome this problem, one possible approach is to integrate functional biological agents or drugs, such as growth factors, into the biomimetic coating [9–11]. Growth factors are proteins that serve as signaling agents for cells and stimulate cellular differentiation, proliferation, migration, adhesion, and gene expression during bone repair, thereby efficiently accelerate bone regeneration [12–15]. Therefore, it is instructive and necessary to incorporate osteogenic agents, such as growth factors, hormones and peptides, into biomimetic coatings.

Currently, osteoinductive proteins, such as bone morphogenetic protein (BMP), have been incorporated into biomimetic coating using two approaches [16, 17]. In the first approach, the osteoinductive agent is directly dropped onto the surface of the biomimetic coating allowing the coating to serve as a delivery carrier. With this method, high protein incorporation efficiency (nearly 100%) is obtained, but the adsorbed agent is liberated too rapidly to

X. Yu · H. Qu · M. Wei (✉)
Department of Chemical, Materials & Biomolecular Engineering, University of Connecticut, 97 North Eagleville Road, U-3136, Storrs, CT 06269, USA
e-mail: m.wei@ims.uconn.edu

D. A. Knecht
Department of Molecular and Cell Biology, University of Connecticut, 91 N. Eagleville Rd, U-3125, Storrs, CT 06269, USA

induce a sustained osteogenic response [18–20]. In the second approach, the osteoinductive protein is added to the SBF solution and co-precipitated with the CaP coating onto the substrate material. In this manner, a more sustained release is achieved [8, 17, 21]. Unfortunately, the protein incorporation rate reported with this method is extremely low, where approximately 3–15% of the proteins in the SBF were incorporated into the CaP coating [17, 22, 23]. This results in a huge waste of the extremely expensive osteoinductive proteins [24–26].

In this study, we attempted to improve the protein incorporation rate by carefully adjusting the substrate surface area to SBF volume ratio (SSA/SV ratio). A low volume of SBF was employed to increase the SSA/SV ratio to assure most of the calcium and phosphate ions in the SBF solution contribute to the coating formation. Bovine serum albumin (BSA) was used as a model protein to co-precipitate with the biomimetic coating onto a titanium substrate. The BSA incorporation rate as well as its subsequent release profiles were investigated.

2 Materials and methods

2.1 Preparation of coating

Commercially available titanium strips (18 mm × 2 mm × 0.5 mm) were used as the substrates in this research. These strips were roughened by #800 sandpaper, follow by an alkaline treatment using 6 M NaOH at 60°C for 24 h. They were then thoroughly washed with de-ionized water, and immersed in a modified SBF solution (m-SBF). The m-SBF solution was prepared based on the procedures described by Oyane et al. [27], but the ion concentrations were adjusted according to Table 1.

BSA was employed as a model protein in the current study, and it was labeled using Alexa488 (Invitrogen, USA). To avoid protein absorption onto the container wall, all the tubes used in this study were pre-coated with 1% non-fluorescent labeled BSA solution for 1 h, and then washed by PBS for three times. The pretreated titanium strip was vertically placed into a 1.5 ml tube (Fisher, USA) containing 1.0 ml m-SBF and BSA. Two Alexa488-BSA concentrations,10 and 100 μg/ml, were studied. The samples were incubated in a water bath at 42°C for 24 h and then removed from the tube, rinsed with deionized water, and air dried at ambient temperature overnight.

Table 1 Inorganic composition of human blood plasma and m-SBF

Ion	Concentration (mM)	
	Blood plasma	m-SBF
K^+	5.0	6.0
Na^+	142.0	370.0
Ca^{2+}	2.5	8.0
Mg^{2+}	1.5	3.0
Cl^-	103.0	376.0
HCO_3^-	27.0	18
SO_4^{2-}	0.5	0
HPO_4^{2-}	1.0	3.0

2.2 Characterization of coating

Field emission scanning electron microscopy (FESEM, JEOL 6335F) was employed to study the surface morphologies of the biomimetic coating with and without BSA incorporation. Infrared spectra were recorded by a Nicolet XS60 Fourier transform infrared (FTIR) spectroscopy. The coating was removed from titanium substrate using a scalpel and subsequently ground into powder for FTIR examination. FTIR spectra were obtained between wavelengths 4,000–400 cm^{-1} at a resolution of 2 cm^{-1} and an average scan of 128 scans. All coatings with and without BSA were examined using an X-ray diffractometer (Siemens D500) with a copper target. The voltage and current settings were 40 kV and 40 mA, respectively. A step size of 0.04° and a scan speed of 0.5°/min were used.

2.3 Incorporation of BSA in the coating

BSA concentrations in m-SBF before and after biomimetic coating process were compared. Briefly, the amount of BSA remaining in the m-SBF after the coating process was measured using a microplate reader (Molecular Devices M2 plate reader, USA) with a fluorescence absorbance mode of an excitation wavelength of 497 nm and emission wavelength of 520 nm. Thus, the BSA incorporation into the coating can be calculated using the following equation:

$$R_{\text{incorporation}}(\%) = \frac{(C_{\text{initial}} - C_{\text{remained}})}{C_{\text{initial}}} \times 100\% \quad (1)$$

where $R_{\text{incorporation}}$ is the BSA incorporation rate into coating, C_{initial} the initial BSA concentration in SBF before coating (amount pre-determined), and C_{remained} is the BSA concentration remained in SBF after coating.

2.4 Efficiency of calcium and phosphate forming into the coating

The initial concentrations of calcium and phosphate in m-SBF were 8.0 and 3.0 mM (pre-determined), respectively. Not all the calcium and phosphate in the SBF participated in the coating formation. The amount of calcium and phosphate participating in the biomimetic coating formation was determined by measuring the remaining calcium and phosphate ion concentrations in the SBF after

coating formation. Similar to the BSA assessment, the efficiency of calcium and phosphate forming into coating was also calculated based on Eq. 1, where $C_{initial}$ is the initial calcium and phosphate concentrations in m-SBF, and $C_{remained}$ is the calcium and phosphate concentrations in m-SBF after coating formation. The calcium concentration in SBF was measured using an atomic absorbance spectrometer (AAS, Perkin Elmer-5000, USA), and the phosphate concentration was determined using molybdenum blue chemistry [28]. For the phosphate measurement, pure water, 2.5 wt% ammonium molybdate, and 10 wt% ascorbic acid (v:v:v = 5:1:1) were added in the above order to form a working solution. The working solution was mixed with the testing solution at a volume ratio of 4:1(v/v), and then incubated at 60°C for 15 min. The mixed solution was subsequently examined using a microplate reader (Biotek, MQX200) at a wavelength of 830 nm.

2.5 In vitro BSA release kinetics

To study protein release kinetics, the biomimetic coated titanium strip with Alexa488-BSA ($n = 4$ for each concentration) was soaked in 1.0 ml phosphate buffered saline (PBS) in a sealed 1.5 ml Eppendorf tube at 37°C for 15 days. At each time point, 1.0 ml of the immersion solution was taken out for Alexa488-BSA concentration measurement. The same volume of PBS was added to the container to maintain a constant volume of the soaking solution. The Alexa488-BSA concentration in each solution was determined as stated in Sect. 2.3.

After 15 days of BSA release, the samples were removed from tubes, rinsed with distilled water and dried at room temperature. The surface morphology of these samples was observed using a FESEM.

3 Results

3.1 Coating characterization

Figure 1 shows FESEM micrographs of the biomimetic coating on a titanium substrate. Incorporation of BSA resulted in morphological changes of the CaP crystals. Both the coatings with and without BSA were composed of CaP crystal plates with a length of approximately 2 μm, but the morphology of the plates changed substantially after the incorporation of BSA. The crystal plates of the coating without BSA were relatively flat with sharp edges, and most of them were well separated from each other (Fig. 1A and B). By contrast, the crystal plates of the coating with BSA were severely bent and contacting with the surrounding crystals in a random manner (Fig. 1C–F). In addition, as the BSA concentration in m-SBF increased from 10 to 100 μg/ml, the extent of bending of the crystals increased as demonstrated in Fig. 1D and F. The obvious differences between these two biomimetic coatings imply that BSA has not only incorporated into the coating, but also affected the lattice structure and orientation of the CaP crystals.

The FTIR spectra of BSA powder, a biomimetic coating without BSA, and biomimetic coatings with BSA at different concentrations are plotted in Fig. 2. The spectra of pure BSA and biomimetic coating are present as controls. The spectrum of the BSA powder exhibited an apparent absorption band at 1,654 cm^{-1} assigned to C=O stretching mode of amide I and 1,540 cm^{-1} assigned to N–H bending mode of amide II. The spectrum of the coating without BSA illustrated three characteristic bands: 1,040 cm^{-1} assigned to P–O stretching mode, and both 602 cm^{-1} and 563 cm^{-1} assigned to O–P–O bending mode. For the coatings with BSA, two bands at 1,654 cm^{-1} and 1,540 cm^{-1} were also observed, suggesting that BSA has incorporated into the biomimetic coating. The bands for the coating with a BSA concentration of 100 μg/ml were more prominent than those with a BSA concentration of 10 μg/ml, suggesting more BSA is incorporated into the former coating than the latter. Nevertheless, the OH stretching band at ~3,572 cm^{-1} was not observed, indicating the coating formed may not be apatite.

Figure 3 shows the X-ray diffraction (XRD) patterns of the BSA-loaded biomimetic coatings. The coatings were identified as octocalcium phosphate (OCP, $Ca_8(HPO_4)_2(PO_4)_4 \cdot 5H_2O$) which exhibits a unique diffraction peak at $2\theta = 4.7°$ corresponding to the (100) plane of OCP. Other peaks appeared at 10°, 16°, 26°, and 32° in the XRD spectra also match with OCP. No considerable difference in those characteristic diffraction peaks was discerned between the coatings with and without BSA.

3.2 BSA incorporation efficiency

The fluorescence associated Alexa488-BSA was used to quantify the incorporation of BSA into the biomimetic coating. About 90% of the BSA (~9 μg) in m-SBF was incorporated into the biomimetic coating when the original BSA concentration was low, such as 10 μg/ml (Fig. 4). When the initial Alexa488-BSA concentration in SBF increased to 100 μg/ml, the loading efficiency decreased to about 60%, which is still much higher than the incorporation rate reported by most researchers [3, 17, 23].

3.3 Calcium and phosphate incorporation efficiency

Calcium and phosphate incorporation rates were also high in both m-SBF solutions with two different BSA concentrations (Fig. 5). Despite of the differences in BSA concentrations in the two solutions, approximately 90% of

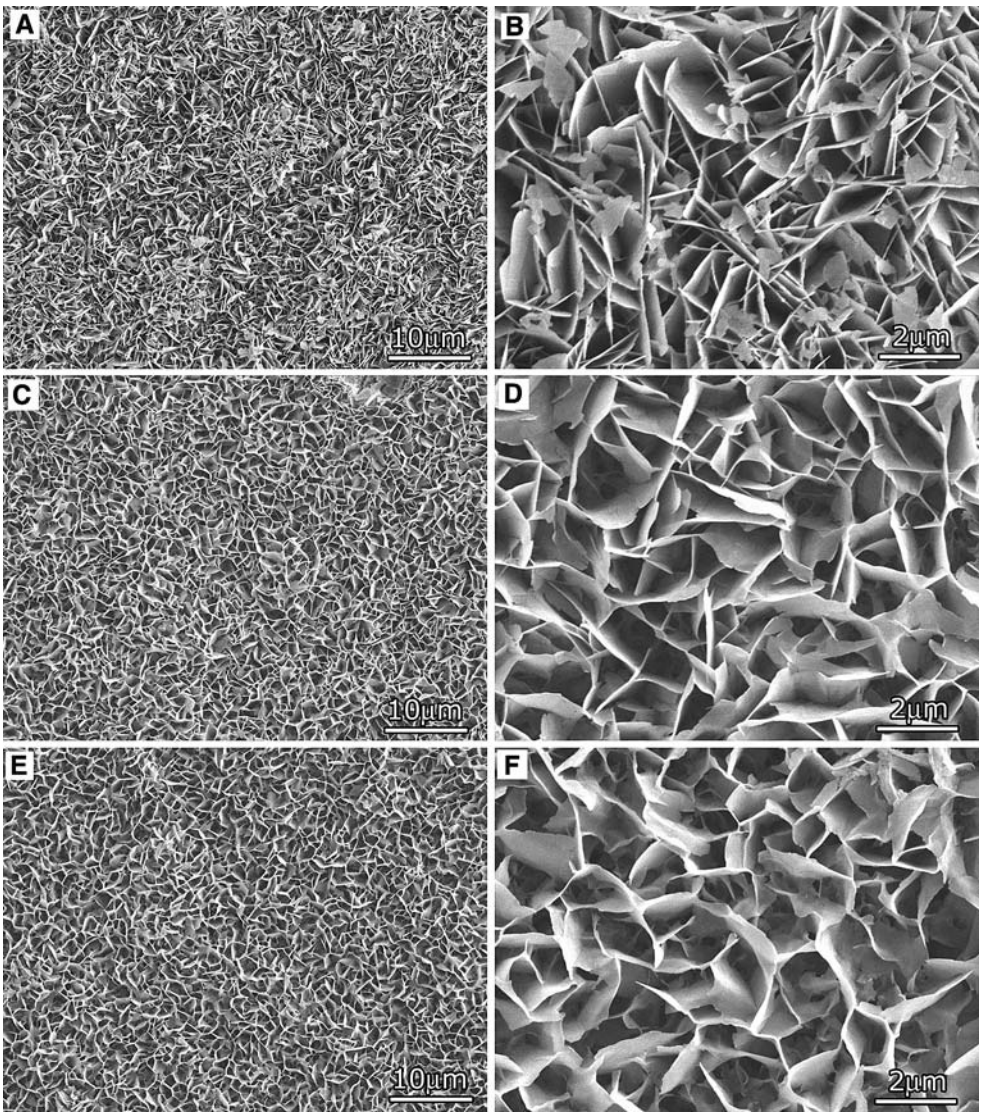

Fig. 1 Scanning electron microscopy micrographs of biomimetic coatings prepared with different BSA concentrations: (**A**) BSA free (2,000×), (**B**) 10 μg/ml BSA (2,000×), (**C**) 100 μg/ml BSA (2,000×), and (**D**) BSA free (10,000×), (**E**) 10 μg/ml BSA (10,000×), and (**F**) 100 μg/ml BSA (10,000×)

the phosphate and 60% of the calcium in the initial m-SBF participated in the biomimetic coating formation in both groups. Apparently, most of the phosphate in the solution was used up to form the coating, while 40% of the calcium still remained in the m-SBF.

3.4 BSA release kinetics

The release profiles of BSA from biomimetic coatings are shown in Fig. 6. For the coating with a BSA concentration of 10 μg/ml, there was hardly any BSA released from the coating after 15 days of immersion in PBS (Fig. 6). By contrast, the BSA release in the coating with a BSA concentration of 100 μg/ml was much faster during the first 12 h of immersion. After the first 12 h, the release of BSA slowed down and a sustained release was observed until the end of the study period (15 days). Basically, about 4 μg BSA was released in a fashion so-called "burst release" in the first 12 h, while about 2.5 μg BSA was released in a sustained mode. The total BSA release from the coating with a BSA concentration of 100 μg/ml was approximately 6.5 μg, which was about 11% of the total amount of BSA incorporated into the coating initially.

3.5 Morphology of the coating after BSA release

The morphology of the coating changed dramatically after BSA release (Fig. 7). The large plate-like porous coating (Fig. 1) disappeared after immersion in PBS for 15 days. Instead, a homogenous dense CaP coating was observed

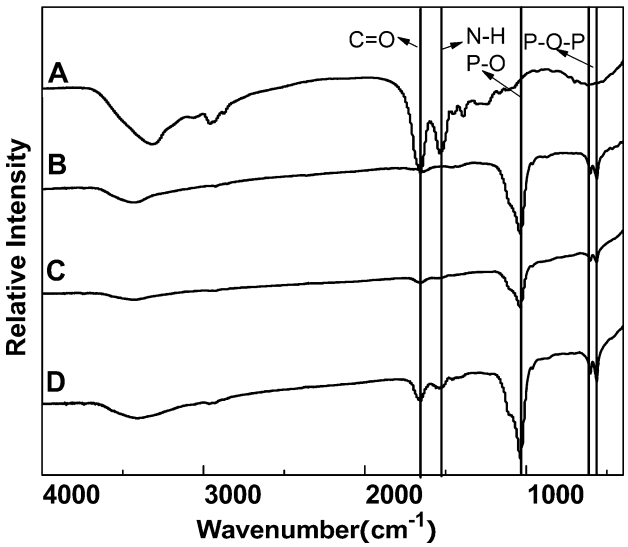

Fig. 2 FT-IR spectra of the biomimetic coating with different BSA concentrations: (**A**) pure BSA, (**B**) biomimetic coating without BSA, (**C**) biomimetic coating with 10 μg/ml BSA, and (**D**) biomimetic coating with 100 μg/ml

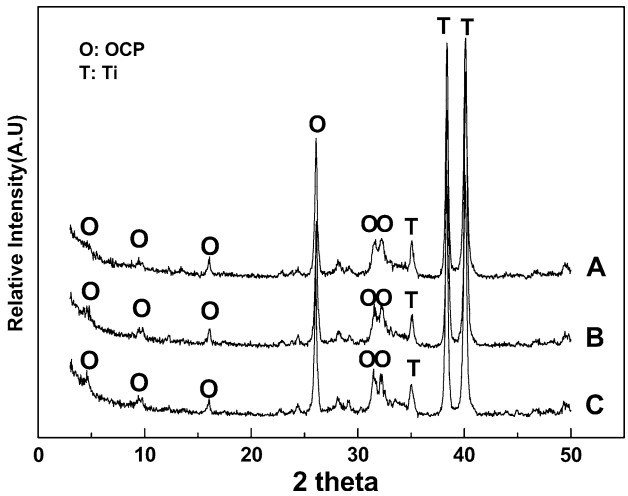

Fig. 3 XRD patterns of the biomimetic coating with different BSA concentrations: (**A**) biomimetic coating without BSA, (**B**) biomimetic coating with 10 μg/ml BSA, and (**C**) biomimetic coating with 100 μg/ml BSA

(Fig. 7). Interestingly, compared to the coating without BSA, a few holes appeared in the coating containing BSA after 15 days of immersion in PBS. More holes were found in the coating with a higher BSA concentration (Fig. 7C and E), which probably indicated that the coating with a higher BSA content might dissolve faster.

4 Discussion

One objective of this study was to markedly improve the efficiency of protein loading during the biomimetic coating

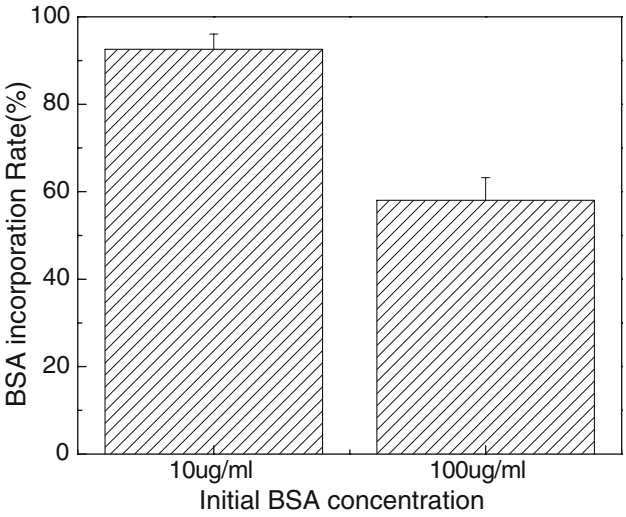

Fig. 4 BSA loading efficiency in biomimetic coating at different BSA concentrations

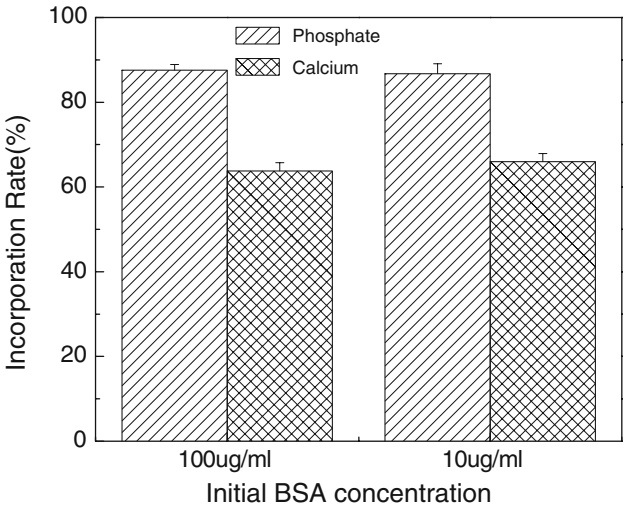

Fig. 5 Calcium and phosphate incorporation efficiencies in biomimetic coatings at different BSA concentrations

processing. CaP coating produced by the biomimetic method has demonstrated the capability of enhancing early-stage bone apposition and long-term fixation of titanium prostheses [29, 30]. Both of our FTIR and XRD results confirmed that OCP coating was formed instead of apatite, which may be due to the high sodium and chloride concentrations employed in our m-SBF. The release behavior of incorporating biomolecules onto/into the biomimetic coating has been investigated [31, 32]. It was found that if the biomolecules were simply adsorbed onto the surface of the coating, a "burst" release of proteins was observed which is not beneficial to the bone healing process [26]. Biomolecules have also been successfully incorporated into CaP coating through a biomimetic

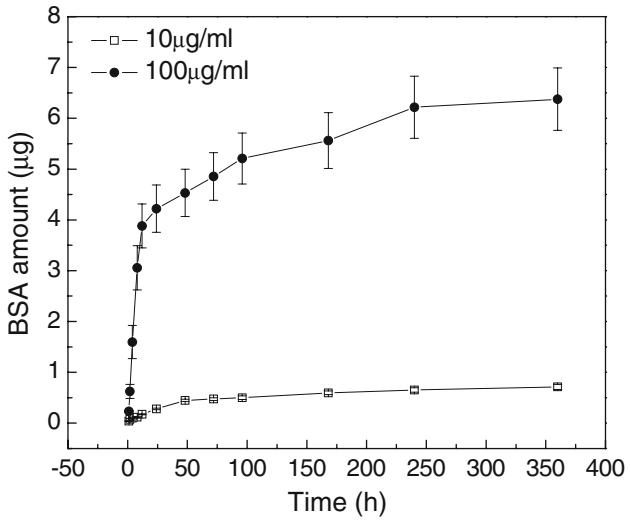

Fig. 6 Cumulative release profiles of BSA from biomimetic coatings with different BSA concentrations: 10 and 100 μg/ml BSA

coating method, and a sustained release was achieved [21]. However, the loading efficiency of the biomolecules into the biomimetic CaP coating was extremely low, approximately 15% [21], leading to a huge waste of the extremely expensive proteins [5, 33, 34]. Drug loss, especially during the loading processing, is one of the most common problems associated with drug delivery systems [35]. The main reason for the low protein incorporation efficiency was the relatively large volume of simulated body fluid used in these studies, 30–200 ml [17, 22, 23]. During the coating formation, only a small amount of calcium, phosphate and protein incorporated into the coating, while excessive minerals and protein remained in the SBF solution. In this study, we increased the SSA/SV ratio up to 0.072, resulting in more than 90% of the phosphate ions and 60% of the calcium ions participated in the coating formation (Fig. 5). Together with calcium and phosphate ions, a high proportion of protein (up to 90%) added to the m-SBF was also incorporated into the biomimetic CaP coating (Fig. 4).

In general, about 30–200 ml SBF is used to produce a CaP coating on an implant [3, 8, 21, 36], which yields an SSA/SV ratio between 0.005 and 0.03. When the SSA/SV ratio is too low, a substantial amount of calcium and phosphate ions as well as proteins remain in SBF after the coating, resulting in a low loading efficiency. On the other hand, if SSA/SV ratio is too high, it becomes difficult to stabilize the SBF and subsequently form biomimetic coating. In this study, the surface area of the specimens is fixed. At a given SSA, we carefully adjusted the SV by selecting containers with appropriate dimensions to minimize the SBF volume used.

It is also known that the BSA incorporation efficiency is closely associated with the proportion of calcium and phosphate ions in the SBF participating in biomimetic CaP coating formation. BSA molecules have special affinity to positive calcium ions through their negatively charged $COOH^-$ terminal groups under a close to neutral pH [37]. The working pH range of m-SBF in our system is between 6.2 and 6.8. Within this pH range, BSA binds to calcium ions on the surface through electrostatic interactions. It gradually incorporates into the CaP coating with calcium and phosphate ions [23, 38]. When the volume of m-SBF is high, only a small proportion of calcium and phosphate in the SBF participate in the coating formation, and the rest together with the excess protein remain in the m-SBF solution. By contrast, if a low volume, e.g. 1.0 ml, of m-SBF is used as demonstrated in the current study, almost all the phosphate ions and a large proportion of calcium ions in the solution are used up to form the coating (see Fig. 6). Since BSA is bonded to calcium phosphate, its incorporation rate increases with the calcium and phosphate incorporation rate. Different loading efficiencies were obtained using various BSA concentrations indicating that it is important to choose an appropriate protein concentration for a certain coating system even though a low m-SBF volume is used. For a given surface area, the amount of protein incorporated is limited. Using an extremely high protein concentration could also lead to a low protein incorporation efficiency. Therefore, it is critical to choose the appropriate SBF volume and BSA concentration to obtain high loading efficiency.

It was found from material characterization that the biomimetic coating formed on the surface of the titanium strip was thin and porous. Also, amide bands were detected by FT-IR (Fig. 2) in the protein-containing coating, implying that BSA has incorporated into the biomimetic coating. The surface morphology of the coating with BSA was significantly different from those without BSA. The heavily bent crystal plates further indicated that the BSA is not simply adsorbed onto the surface of the coating [26, 38]. Instead, BSA has been incorporated into the lattice structure of the CaP coating through the electrostatic interactions between BSA and the mineral [37, 39, 40].

The cumulative release profiles of BSA from the biomimetic coatings suggest that most of BSA was trapped in the coating after 15 days of immersion in PBS. This was due to the fact that BSA was chemically bonded to CaP crystal plates rather than simply adsorbed onto the surface of the coating, so the bonding between the CaP crystals and BSA was strong. For the coating prepared with 100 μg/ml BSA, about 11% BSA was released during the subsequent immersion. Meanwhile, it was found that part of the coating dissolved, and left many holes in the coating. These results collectively imply that the release of BSA may be controlled by both diffusion and dissolution of the biomimetic coating. Although most of the BSA remained in the

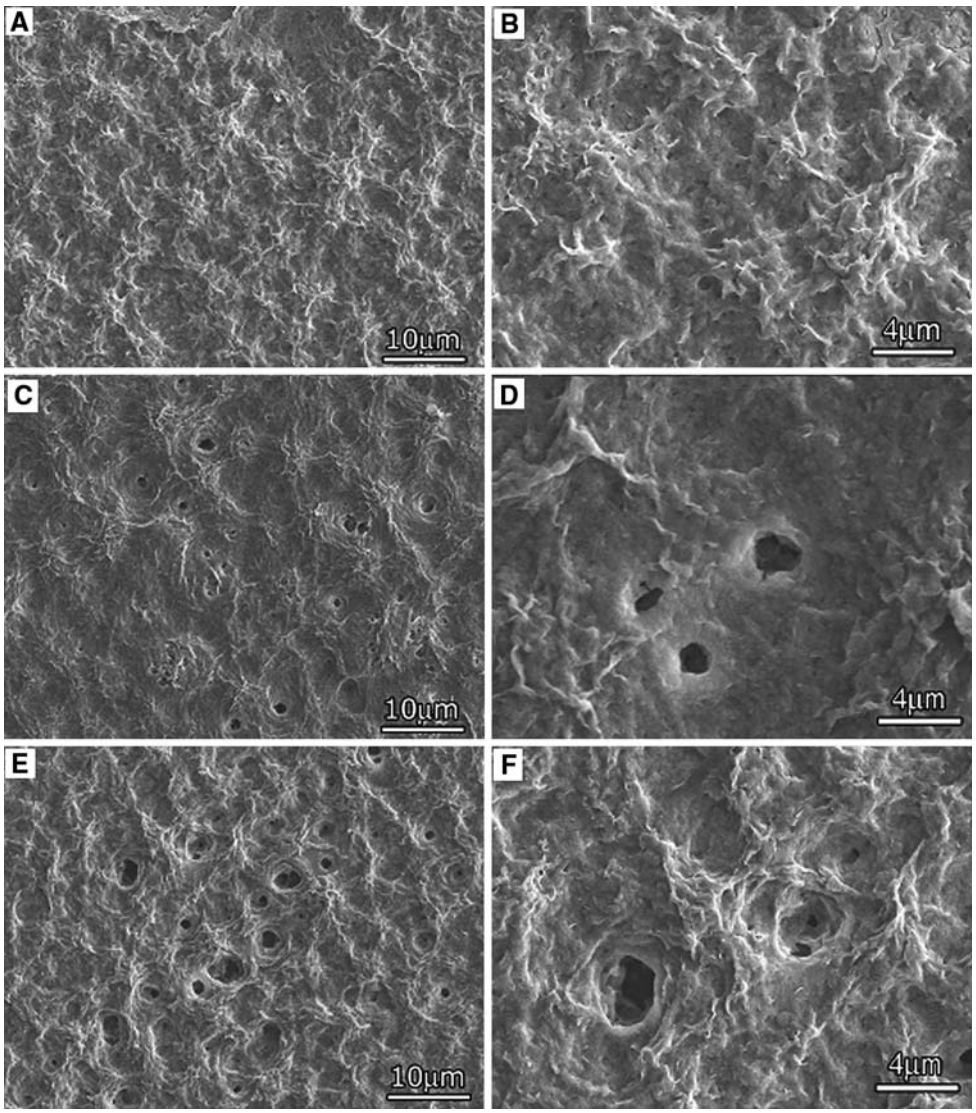

Fig. 7 Scanning electron microscopy micrographs of biomimetic coatings with different BSA concentrations after 15 days immersion in deionized water: (**A**) BSA free (2,000×), (**B**) BSA free (5,000×), (**C**) 10 μg/ml BSA (2,000×), (**D**) 10 μg/ml BSA (5,000×), (**E**) 100 μg/ml BSA (2,000×), and (**F**) 100 μg/ml BSA (5,000×)

coating, it has been reported that the protein could be released at a much faster rate in vivo due to the faster degradation rate of the coating at physiological conditions [17]. In addition, our previous study also demonstrated that the biomimetic CaP coating properties, such as density and crystallinity, can be tailored by adjusting the pH, volume and ionic strength of SBF [41, 42], and the coating density and crystallinity have direct impact on the coating degradation rate. Chou et al's study also showed that the pH of SBF had a clear influence on the morphology and crystallinity of the coating [43]. Ionic strength of SBF was also shown to affect the density and crystallinity of the coating [2]. Therefore, the protein release profiles from the biomimetic CaP coating can also be adjusted by tailoring the coating density and crystallinity and in turn varying the degradation of the CaP coating.

It was also found that the crystallinity of the coating was significantly altered after the 15 days of immersion. Our previous study suggested that the coating formed on titanium substrate has a gradient structure with a dense, low crystalline coating adjacent to the substrate to form a strong bonding and a porous, large crystalline top surface to facilitate tissue ingrowth. As a result, before incubation in PBS, the coating surface exhibited a highly crystalline structure (Fig. 1). After the 15 days incubation, the top layer of the coating was dissolved, and the bottom layer of the coating was revealed which had a much finer and denser structure than that on the surface (Fig. 7).

5 Conclusions

BSA was employed as a model protein to be incorporated into a calcium phosphate coating using a biomimetic method. A high incorporation rate (>90%) was achieved by dramatically reducing the SBF volume used for immersion the metallic substrate. It was found that the BSA was successfully incorporated into the biomimetic coating and resulted in a significant change in crystal morphology and composition. In the subsequent release study, a sustained release was achieved for the coating containing 100 μg/ml BSA. In summary, our results suggest that co-precipitation is a promising method of incorporating osteoinductive agents into calcium phosphate coatings, resulting in a coating with both osteoconductive and osteoinductive properties.

Acknowledgements The authors would like to thank the supports from National Science Foundation (DMI 0500269 and BES 0503315) and Connecticut Innovations under the Yankee Ingenuity Technology Competition.

References

1. T. Kokubo, Acta Mater. **46**, 2519 (1998). doi:10.1016/S1359-6454(98)80036-0
2. F. Barrere, C.A. van Blitterswijk, K. de Groot, P. Layrolle, Biomaterials **23**, 1921 (2002). doi:10.1016/S0142-9612(01)00318-0
3. Y. Liu, P. Layrolle, J. de Bruijn, C. van Blitterswijk, K. de Groot, J. Biomed. Mater. Res. **57**, 327 (2001). doi:10.1002/1097-4636(20011205)57:3<327::AID-JBM1175>3.0.CO;2-J
4. F. Barrere, M.M. Snel, C.A. van Blitterswijk, K. de Groot, P. Layrolle, Biomaterials **25**, 2901 (2004). doi:10.1016/j.biomaterials.2003.09.063
5. P. Habibovic, F. Barrere, C.A. van Blitterswijk, K. de Groot, P. Layrolle, J. Am. Ceram. Soc. **85**, 517 (2002)
6. P. Habibovic, C.M. van der Valk, C.A. van Blitterswijk, K. de Groot, G. Meijer, J. Mater. Sci. Mater. Med. **15**, 373 (2004). doi:10.1023/B:JMSM.0000021104.42685.9f
7. F. Barrere, C.M. van der Valk, R.A. Dalmeijer, G. Meijer, C.A. van Blitterswijk, K. de Groot et al., J. Biomed. Mater. Res. A **66**, 779 (2003). doi:10.1002/jbm.a.10454
8. C. Du, G.B. Schneider, R. Zaharias, C. Abbott, D. Seabold, C. Stanford et al., J. Dent. Res. **84**, 1070 (2005)
9. H. Schliephake, A. Aref, D. Scharnweber, S. Bierbaum, S. Roessler, A. Sewing, Clin. Oral. Implants Res. **16**, 563 (2005). doi:10.1111/j.1600-0501.2005.01143.x
10. A. Krout, H. Wen, E. Hippensteel, P. Li, J. Biomed. Mater. Res. A **73**, 377 (2005). doi:10.1002/jbm.a.30310
11. Y. Liu, K. de Groot, E.B. Hunziker, Bone **36**, 745 (2005). doi:10.1016/j.bone.2005.02.005
12. E. Solheim, Int. Orthop. **22**, 410 (1998). doi:10.1007/s002640050290
13. R.O. Oreffo, Curr. Opin. Investig. Drugs **5**, 419 (2004)
14. J.R. Lieberman, A. Daluiski, T.A. Einhorn, J. Bone Joint Surg. Am. **84**, 1032 (2002)
15. V. Luginbuehl, L. Meinel, H.P. Merkle, B. Gander, Eur. J. Pharm. Biopharm. **58**, 197 (2004). doi:10.1016/j.ejpb.2004.03.004
16. R. Vasita, D.S. Katti, Expert Rev. Med. Devices **3**, 29 (2006). doi:10.1586/17434440.3.1.29
17. Y. Liu, R.O. Huse, K. de Groot, D. Buser, E.B. Hunziker, J. Dent. Res. **86**, 84 (2007)
18. J.O. Hollinger, K. Leong, Biomaterials **17**, 187 (1996). doi:10.1016/0142-9612(96)85763-2
19. A.H. Reddi, Tissue Eng. **6**, 351 (2000). doi:10.1089/107632700418074
20. J.W. Vehof, H. Takita, Y. Kuboki, P.H. Spauwen, J.A. Jansen, J. Biomed. Mater. Res. **61**, 440 (2002). doi:10.1002/jbm.10216
21. H. Wen, J.R. de Wijn, C.A. van Blitterswijk, K. de Groot, J. Biomed. Mater. Res. **46**, 245 (1999). doi:10.1002/(SICI)1097-4636(199908)46:2<245::AID-JBM14>3.0.CO;2-A
22. Y. Liu, E.B. Hunziker, P. Layrolle, J.D. de Bruijn, K. de Groot, Tissue Eng. **10**, 101 (2004). doi:10.1089/107632704322791745
23. L.N. Luong, S.I. Hong, R.J. Patel, M.E. Outslay, D.H. Kohn, Biomaterials **27**, 1175 (2006). doi:10.1016/j.biomaterials.2005.07.043
24. Y. Liu, J. Li, E.B. Hunziker, K. de Groot, Philos. Trans. R. Soc. A-Math. Phys. Eng. Sci. **364**, 233 (2006). doi:10.1098/rsta.2005.1685
25. Y. Liu, E.B. Hunziker, P. Layrolle, C. Van Blitterswijk, P.D. Calvert, K. de Groot, J. Biomed. Mater. Res. A **67**, 1155 (2003). doi:10.1002/jbm.a.20019
26. Y. Liu, K. de Groot, E.B. Hunziker, Ann. Biomed. Eng. **32**, 398 (2004). doi:10.1023/B:ABME.0000017536.10767.0f
27. A. Oyane, H.M. Kim, T. Furuya, T. Kokubo, T. Miyazaki, T. Nakamura, J. Biomed. Mater. Res. A **65**, 188 (2003). doi:10.1002/jbm.a.10482
28. S. Karthikeyan, S. Hashigaya, T. Kajiya, S. Hirata, Anal. Bioanal. Chem. **378**, 1842 (2004). doi:10.1007/s00216-004-2501-9
29. P. Li, J. Biomed. Mater. Res. A **66**, 79 (2003). doi:10.1002/jbm.a.10519
30. D.H. Kohn, S.J. Hollister, K.E. Healy, J. Dent. Res. **79**, 144 (2000)
31. R.F.S. Lenza, J.R. Jones, W.L. Vasconcelos, L.L. Hench, J. Biomed. Mater. Res. A **67A**, 121 (2003). doi:10.1002/jbm.a.10042
32. J.E. Barralet, S. Aldred, A.J. Wright, A.G.A. Coombes, J. Biomed. Mater. Res. **60**, 360 (2002). doi:10.1002/jbm.10070
33. P. Li, P. Ducheyne, J. Biomed. Mater. Res. **41**, 341 (1998). doi:10.1002/(SICI)1097-4636(19980905)41:3<341::AID-JBM1>3.0.CO;2-C
34. H.K. Varma, Y. Yokogawa, F.F. Espinosa, Y. Kawamoto, K. Nishizawa, F. Nagata et al., Biomaterials **20**, 879 (1999). doi:10.1016/S0142-9612(98)00243-9
35. L.W. Chan, X. Liu, P.W.S. Heng, J. Microencapsul. **22**, 891 (2005). doi:10.1080/02652040500273936
36. M. Stigter, J. Bezemer, K. de Groot, P. Layrolle, J. Control. Release **99**, 127 (2004). doi:10.1016/j.jconrel.2004.06.011
37. D.T.H. Wassell, R.C. Hall, G. Embery, Biomaterials **16**, 697 (1995). doi:10.1016/0142-9612(95)99697-K
38. T.Y. Liu, S.Y. Chen, D.M. Liu, S.C. Liou, J. Control. Release **107**, 112 (2005). doi:10.1016/j.jconrel.2005.05.025
39. S. Shimabayashi, Y. Tanizawa, K. Ishida, Chem. Pharm. Bull. (Tokyo) **39**, 2183 (1991)
40. D.I. Hay, E.C. Moreno, J. Dent. Res. **58**, 930 (1979)
41. H. Qu, M. Wei, J. Biomed. Mater. Res. B Appl. Biomater. **84B**, 436 (2008). doi:10.1002/jbm.b.30889
42. H. Qu, M. Wei, Key. Eng. Mater. **330–332**(2), 757 (2007)
43. Y.F. Chou, W.A. Chiou, Y. Xu, J.C. Dunn, B.M. Wu, Biomaterials **25**, 5323 (2004)